energies

MDPI

Article

Melanopic Limits of Metamer Spectral Optimisation in Multi-Channel Smart Lighting Systems

Babak Zandi *, Adrian Eissfeldt, Alexander Herzog and Tran Quoc Khanh

Laboratory of Lighting Technology, Department of Electrical Engineering and Information Technology, Technical University of Darmstadt, D-64289 Darmstadt, Germany; eissfeldt@lichttechnik.tu-darmstadt.de (A.E.); herzog@lichttechnik.tu-darmstadt.de (A.H.); khanh@lichttechnik.tu-darmstadt.de (T.Q.K.)
* Correspondence: zandi@lichttechnik.tu-darmstadt.de

Abstract: Modern indoor lighting faces the challenge of finding an appropriate balance between energy consumption, legal requirements, visual performance, and the circadian effectiveness of a spectrum. Multi-channel LED luminaires have the option of keeping image-forming metrics steady while varying the melanopic radiance through metamer spectra for non-visual purposes. Here, we propose the theoretical concept of an automated smart lighting system that is designed to satisfy the user's visual preference through neural networks while triggering the non-visual pathway via metamers. To quantify the melanopic limits of metamers at a steady chromaticity point, we have used 561 chromaticity coordinates along the Planckian locus (2700 K to 7443 K, $\pm Duv$ 0 to 0.048) as optimisation targets and generated the spectra by using a 6-channel, 8-channel, and 11-channel LED combination at three different luminance levels. We have found that in a best-case scenario, the melanopic radiance can be varied up to 65% while keeping the chromaticity coordinates constant $\left(\Delta u'v' \leq 7.05{\times}10^{-5}\right)$ by using metamer spectra. The highest melanopic metamer contrast can be reached near the Planckian locus between 3292 and 4717 K within a Duv range of -0.009 to 0.006. Additionally, we publish over 1.2 million optimised spectra generated by multichannel LED luminaires as an open-source dataset along with this work.

Keywords: smart lighting; multi-channel LED optimisation; circadian photoentrainment; non-image-forming vision; metamer spectra

Citation: Zandi, B.; Eissfeldt, A.; Herzog, A.; Khanh, T.Q. Melanopic Limits of Metamer Spectral Optimisation in Multi-Channel Smart Lighting Systems. *Energies* **2021**, *14*, 527. https://doi.org/10.3390/en14030527

Received: 20 December 2020
Accepted: 17 January 2021
Published: 20 January 2021

1. Introduction

The required illumination parameters for designing indoor lighting systems are visual photometric quantities such as illuminance, approximated brightness metrics, and colour rendering, which serve to optimise the visual performance. In 1924, the international commission on illumination (CIE) defined the spectral luminous efficiency function V(λ) to describe the effectiveness of spectral power distributions X(λ) [1,2]. By integrating a V(λ)-weighted radiation spectrum X(λ), photometric quantities like the luminance L or illuminance E can be derived. Based on European standards, office environments need, at least, an average illuminance of 500 lx in occupied and 300 lx in unoccupied workplaces [3]. However, V(λ) represents the visual pathway's achromatic L + M channel, propagating this fact to the photometric quantities [4,5]. Thus, most indoor illumination systems' light intensity is traditionally adapted to the achromatic luminance channel consisting of L-cones and M-cones.

An ideal efficient static illumination meets the legal requirements and at the same time, saves energy to reduce the operating costs of a lighting system. One of the most straightforward strategies of having a high luminous efficacy of radiation [6] (LER) is to adapt the spectral power distribution to V(λ) through an optimised phosphor-coat mixture of a blue-LED chip while maintaining an appropriate colour rendition. In this way, a higher illumination level can be achieved with less energy consumption compared to non-fitted spectra. However, in the era of smart lighting systems, an additional amount of energy can

be saved by supplying the illumination system with occupancy or light sensor data [3]. As a result, the illumination is dimmable or can be switched off automatically when sufficient daylight is available, or the workplace is unoccupied [7–9]. Recent studies revealed that through an optimised smart lighting system energy costs of 17 to 60% [7] can be saved compared to traditional static lighting solutions [7,10,11]. Besides the aspect of saving energy, research is focusing on the implementation of dynamic patterns of light exposure [12], which vary the illumination or the correlated colour temperature (CCT) to support the circadian rhythm [13] or task-related performance [12]. The discovery of intrinsically photosensitive ganglion cells (ipRGCs) [14–18] made clear that besides the image-forming properties of colour and brightness perception [19], the composition of a light spectrum [20] can also affect the human alertness and cognitive performance [6,21–23]. In the outer retina, six subtypes of ipRGCs (M1 to M6) can be distinguished, each with unique morphological, functional and physiological properties projecting to different targets in the brain [24–31]. The M1-subtype of the ipRGCs directly innervates specific regions of the suprachiasmatic nucleus (SCN) and olivary pretectal nucleus (OPN) to modulate the non-image-forming mechanism involving the circadian photoentrainment and temporal pupil light constriction [15,18,32–37]. In the inner retina, M1-ipRGC dendrites stratify in the outermost sublamina of the inner plexiform layer (IPL), receiving extrinsic synaptic input from rods, L + M-on and inhibitory S-cone signals [26,28,38–46]. The ipRGCs have led to the idea that for impacting biological processes effectively, it is not sufficient to adopt a light spectrum to the image-forming pathway using $V(\lambda)$ together with colour quality metrics as a condition. To support the circadian system, a spectral power distribution needs to have a spectral proportion in the short-wavelength range [31,47–52]. According to a recent work of Brown [53], the melanopic illuminance [54,55] seems to be the best predictor for describing non-visual effects [53], although the M1-ipRGCs receive synaptic time-variant weighted inputs from L-, M-, and S-cones [39,43,56,57].

Modern indoor lighting faces the challenge of finding an appropriate balance between legal requirements, energy-saving, visual performance and non-visual impact [6,58–61]. In this context, multi-channel LED luminaires are of interest because such systems can vary spectra over time to address different visual or non-visual processes precisely [7,62,63]. Multi-channel LED systems are already established as a tool in vision research for triggering different retinal photoreceptor types to detect light-induced physiological or cognitive responses [44,64]. Additionally, the higher degree of freedom in optimising spectra makes metamer stimuli possible, meaning different spectral power distributions at steady luminance and chromaticity coordinates [65]. For instance, metamer spectra can keep image-forming metrics steady while varying the melanopic excitation for non-visual purposes, offering the possibility to optimise stimuli with a minimum and maximum melanopsin signal. The circadian system can be influenced actively with such stimuli, depending on the melanopic radiance contrast between two metamer spectra [23,66,67].

Regardless of the technical implementation of an illumination system, there are two possible approaches to implement the neurophysiological findings in automated interior lighting systems. First, study results from visual and non-visual investigations can be used to provide users with a periodic illumination pattern with a recommended spectral distribution throughout the day [12]. Such fully automated lighting systems can either adapt to daylight in terms of CCT or run a pre-set of an ideal illumination pattern with respective melanopic excitation. One drawback is that users could not participate in the automation, which can lead to unsatisfaction or reduced usage of such a system [68–72]. Furthermore, the humans' non-image-forming sensitivity or the visual preference of a correlated colour temperature and illuminance varies between individuals and cannot be managed by an averaged population function alone [73–75]. The approach of a personalised [76] data-driven lighting control through reinforcement learning or neural networks could consider such individual user needs, which adapts to the user's preferences while offering the possibility of correcting model recommendations via a feedback system [68,77–79]. However, previous works did not propose a concept of how non-visual metrics could be handled in a data-driven intelligent lighting system because most users are probably more interested in adjusting visual metrics

like CCT or luminance. In such a data-driven non-parametric approach, this could mean that the melanopic radiance is only indirectly modelled via the CCT without employing the value of metamer spectra. From a practical point of view, a user may prefer a high CCT, but physiologically a low melanopic effect may be recommended at a given time, which could be managed by metamer spectra [23].

Here we have investigated which maximum melanopic radiance contrasts are reachable with metamer spectra using multi-channel LED luminaires. We report the degree of freedom in varying the melanopic radiance at steady chromaticity coordinates and luminance. For this purpose, we have calculated over 1.2 million using 561 chromaticity coordinates as optimisation targets [80], which were located along the Planckian locus (2700 K to 7443 K) for $\pm Duv$ 0 to 0.048. We used 6-channel, 8-channel, and 11-channel LED combination at the luminance levels 140 cd/m^2, 180 cd/m^2 and 220 cd/m^2 for optimisation. Our results reveal the impact of the number of channels and the luminance on the amount of reachable melanopic contrast using metamer spectra. We provide recommendations at which CCTs, chromaticity coordinates and *Duv* to the Planckian locus a higher metamer contrast can be expected, using multi-channel LED luminaires. The knowledge of the melanopic metamer dynamic is essential for future smart lighting systems that utilise multi-channel LED luminaires because metamers could be an effective way to vary non-image-forming parameters. In the first part of this work, we discuss recent studies on intelligent office lighting and propose a theoretical smart lighting concept in which metamer spectra can automatically trigger the non-image-forming pathway without the user's intervention. The second section deals with the performed spectral metamer optimisation results, revealing the limits of the melanopic contrasts along the Planckian locus.

2. The Role of Metamer Spectra in Personalized Smart Lighting Systems

Historically, smart lighting deals with the connection of environmental data to illumination modules for an improved lighting control system, aiming to save energy in office buildings [6,72]. Automated lighting with occupancy and light sensors has proven to be beneficial for energy savings as the illumination is dimmable when there is sufficient daylight or the workplace is unoccupied [72,81–83]. Considering additional information sources for an illumination system requires more effort to design the lighting modules, depending on their degree of integration. For instance, when using a combination of daylight harvesting and artificial light sources to illuminate an office environment, the occupants' workplace lighting needs to be controlled by adjusting the luminaire's dimming level depending on the incoming natural light intensity. In general, a distinction must be made between open-loop and closed-loop control when harvesting daylight for office lighting [84]. In the open-loop approach, only the daylight contribution is measured without capturing the artificial light's illumination proportion. The necessary dimming level of the artificial indoor lighting is either estimated or the light is completely switched off when a threshold is reached at the outdoors's daylight sensor. Closed-loop control systems measure the daylight contribution and the artificial lighting's illuminance to reach a time-dependent dimming control, aiming for a constant and uniform illumination level at the workplace. For this, an outdoor daylight sensor and additional photodetectors placed near the luminaire and the occupants' working area are needed. In most closed-loop systems, occupancy sensors are integrated to dim the lights or switch them off when the workplace is unoccupied. Such an interaction between sensor information and artificial interior lighting is designed to ensure energy saving at the cost of an increased effort in developing the lighting control.

The technological challenge is to control individual lighting modules in different areas to adjust the illumination level dependent on the state of occupancy sensors, blinds and photodetectors placed at several positions [72,84–86]. For this, gradient-based or heuristic optimisation methods are proposed to adapt the dimming level of the luminaire's dependent on environmental sensors via an objective function that integrates at least the energy

cost and legal requirements [83,84,87]. A disadvantage of using optimisation frameworks in a lighting controller, which evaluates additional sensor input data, is the processing time and the scalability for larger office lighting systems [84,88]. Recent works developed new approaches based on neural networks to replace classical optimisation frameworks in closed-loop lighting control units, appealing with scalability and reduced computation time [78,79,84,89]. Incorporating environmental sensors into a fully automated lighting system can minimise energy consumption at the expense of user acceptance, as individual lighting preferences are not considered. Recent studies showed that when users are equipped with the option of overriding an automated lighting system, the illumination is frequently changed according to the user's satisfaction [69,72,90]. The results indicate that energy optimised illumination could be contrary to the preferred lighting condition [72]. Additionally, automated lighting controls which included a feedback system contribute to the user's acceptance [72]. Therefore, past works have considered individual preferences using non-parametric approaches by including sensor data and the user's illumination adjustment behaviour to develop a personalised lighting control through a feedback system that simultaneously incorporates energy consumption [3,68,77,78]. However, recent works used single-channel luminaires and mainly modelled illumination level preferences without considering colourimetric quantities or the feature of metamer spectra. In Figure 1, we have designed the basic structure of a possible intelligent lighting system that could take into account both user preferences and the circadian photoentrainment via metamer spectra. To integrate individual preferences in a self-learning, non-parametric model approach, a user interface [68] must be available to catch the user's light metric adjustments $M_U(t)$ over time t (Figure 1, block 1).

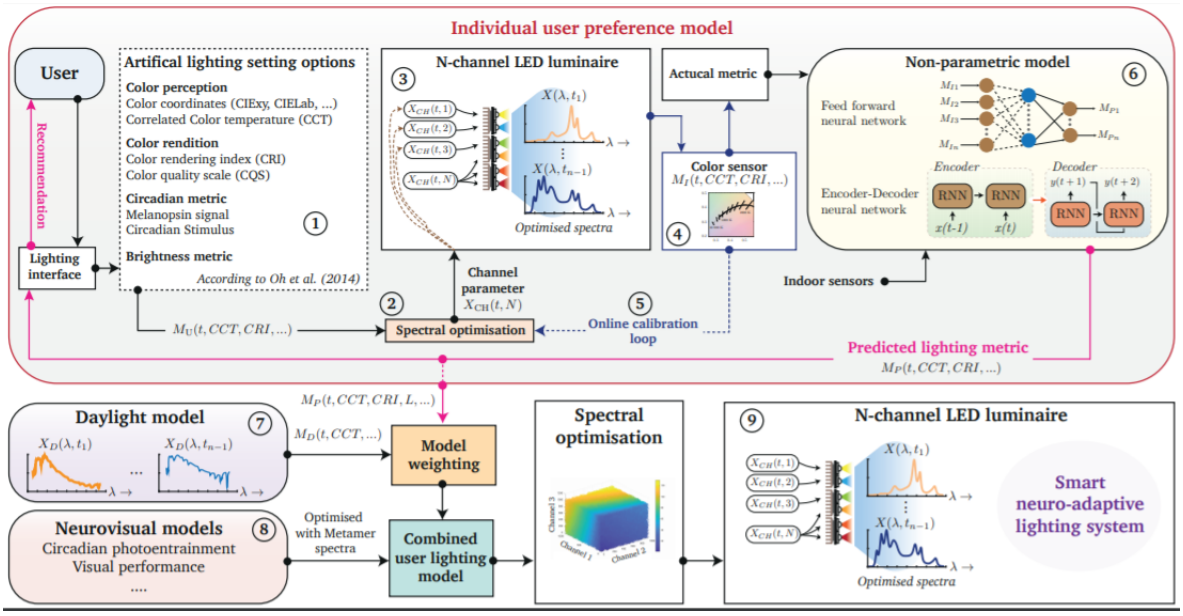

Figure 1. Concept of a self-learning neuro-adaptive smart lighting systems which include metamer spectra for supporting the circadian system. The proposed concept could include three units: An individual user model, a daylight model and neuro-visual models. The user model can be modelled using non-parametric approaches such as neural networks or reinforcement learning to adapt the interior lighting to the user's light adjustment pattern. For training the model, data from a graphical user interface can be used to set lighting metrics. With an appropriate database, the model could provide automated lighting recommendations that can be corrected by the user to improve the preference model within a self-learning cycle. Such a user model only manages the image-forming lighting preferences without considering the energy-saving or circadian effectiveness. Therefore, a daylight model can be used to weight the user model in terms of energy saving for open-loop lighting. Neuro-visual models can be used to increase the melanopic effectiveness of a spectrum by using metamer spectra without impacting the user's image-forming lighting preferences.

Next, each LED-channel values X_{CH} need to be calculated using a spectral optimisation method, such that the condition of the user's light metrics $M_U(t_0)$ is met [58,91] (Figure 1, block 2, 3). During the spectral optimisation, a light sensor or spectrometer can be integrated for online measurements, which checks whether the optimisation tolerances are met [7] (Figure 1, block 4, 5). Subsequently, the optimised light metrics can feed into a user model as feedback data set. In this way, an existing non-parametric user model can be adapted to the user's preferences to make individual recommendations for a light setting $M_P(t_{n+1})$ possible (Figure 1, block 6). If office lighting is automated solely based on individual user preferences, it is expected that energy consumption will not be fully taken into account. Energy can be saved effectively if the illumination level is coupled to the user's occupancy and the proportion of daylight that is integrated into the lighting concept through photodetectors at the window. In this way, artificial lighting can be dimmed when the proportion of daylight is high enough to satisfy the user's preference and legal requirements. The integration of such an energy component can be achieved by weighting the individual user model with a daylight model or a light sensor, which offers the possibility of adapting the CCT from the artificial lighting closer to daylight. The advantage is that the transition between daylight usage and dimming the indoor illumination is not disturbing for observers (Figure 1, block 7). For this, the predicted light setting $M_P(t,\ CCT,\ CRI,\ L,\ \ldots)$ from the individual user model can be merged with a daylight model or data. CRI denotes the colour rendering Index R_a and L the luminance. Kandasamy et al. [78] proposed such a closed-loop lighting approach, which balances out the individual user preference with the amount of daylight that illuminates the workplace. However, a weighted individual user model mainly considers the image-forming metric without actively adjusting the ipRGC stimulation. We assume that metamer spectra will gain attention in personalised lighting solutions, as circadian metrics can be adjusted without affecting the user's image-forming metrics (Figure 1, block 8). For this, metamer spectra can be set automatically based on research recommendations and run in parallel with the individual user model. However, the idea of using metamer spectra in a multi-channel smart lighting system, requires knowledge about the range in which the melanopic signal can be adjusted at constant image-forming metrics.

3. The Melanopic Limits of Metamer Spectra

With multi-channel LED luminaires, it is possible to create N metamer spectra $\{X_i(\lambda)\}_{i=1}^{N}$ with the same luminance L and chromaticity coordinate in the CIExy-2° colour space. Intuitively, one assumes that the luminaire's channel count correlates positively with the possible number N of metamer spectra, due to the higher degree of freedom in mixing individual LED spectra. In this work, we are interested in how much the circadian response of metamer spectra varies when the luminance and CIExy-2° chromaticity coordinates are steady. For this purpose, we optimised metamer spectra $X_i(\lambda)$ and calculated the corresponding melanopsin excitation $L_{Mel,\,i} = \int_{380}^{780} X_i(\lambda) \times s_{mel}(\lambda)\ d\lambda$, with $s_{mel}(\lambda)$ as the melanopic action spectrum [54,55]. For this, chromaticity coordinates must be selected for which the metamer spectra can be optimised. It can be assumed that the adjusted user spectra could converge to the preferred chromaticity coordinates in a personalised smart lighting system. Studies about indoor colour perception revealed that observers tend to prefer spectra with higher chroma [92]. Whereby the reported preferred correlated colour temperatures are between 4000 and 6500 K [93,94]. Previous studies showed that the preferred chromaticity coordinates lie mostly below the Planckian locus. However, the preferred chromaticity points move closer to Planck with increasing CCT. Wang and Wei [95] found that at 3000 K, the preferred chromaticity coordinates have a distance to Planck of Duv −0.02 and −0.03. Whereas with a higher CCT such as 6500 K, the preferred chromaticity points are closer to Planck with a Duv between 0 and −0.01 [95]. This is justified by the fact that chromaticity coordinates below Planck achieve with a higher probability a greater chroma while maintaining the colour fidelity [96]. Thus, chromaticity coordinates directly on Planck, above and below it are of interest for our work. The CCTs

between 2700 and 7000 K are of particular interest, as most studies on indoor lighting have selected chromaticity coordinates in this range [94,95,97]. Therefore, we used 561 chromaticity coordinates along the Planckian locus between 2700 and 7443 K $\pm Duv$ 0 to 0.048 as optimisation targets, reused from a recent publication by Truong et al. [80] (Figure 2a). Truong et al. provides the chromaticity targets in the CCT range of our interest with a sufficiently high span above and below the Planckian locus. An advantage of the higher *Duv* range in the Truong et al. dataset is that the optimised spectra can be studied in relation to the systematic behaviour between the melanopic effectiveness and the distance to Planck. Our initial hypothesis is that chromaticity coordinates below the Planckian locus reach a higher melanopic radiance, but a colour fidelity optimisation criterion could influence this. Furthermore, it is unknown how this could behave with metamer spectra, i.e., whether spectra located below the Planck would achieve a higher melanopic metamer contrast at a steady chromaticity coordinate. We optimised metamer spectra for each of the available chromaticity coordinate (Figure 2a) at the luminance's 140 cd/m^2, 180 cd/m^2, and 220 cd/m^2. The optimisation procedures were performed using a 6-channel, 8-channel, and 11-channel luminaire. We did not change the luminaire itself, but the available LED channels were specified in the optimisation procedure (Figure 2b).

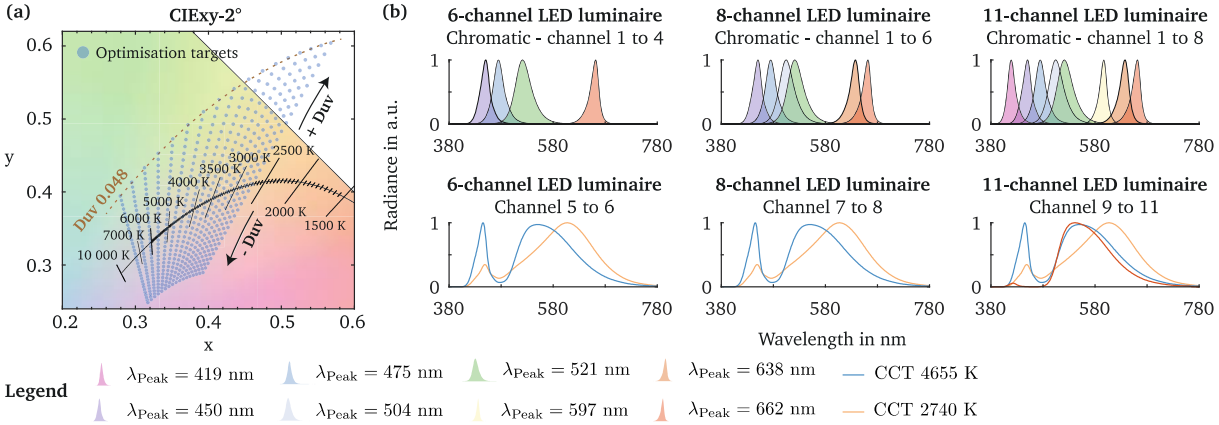

Figure 2. Optimisation targets in the CIExy-2° colour space and the base spectra of the used multichannel LED luminaire to mix the metamers (**a**). As optimisation target, we used chromaticity coordinates along the Planckian locus between 2700 to 7443 K distributed across $\pm Duv$ 0 to 0.048 from a recent publication by Truong et al. (**b**) We mixed the spectra with a 6-channel, 8-channel, and 11-channel luminaire, in which the number of available LEDs was simulated by providing only a certain number of channels as a dependent parameter in the spectral optimisation procedure. The spectra were measured using a Konica Minolta CS-2000 spectroradiometer.

We generated the spectra using a custom-developed heuristic optimisation procedure, which can calculate numerous metamers. For each target condition, spectra were optimised in a loop until a certain number of results were available or the maximum computation time was exceeded, ensuring that sufficient metamers were calculated. The chromaticity targets at low CCTs move beyond the spectrum locus, as these were generated symmetrically by Truong et al. with fixed *Duv* step sizes. We did not pre-filter these outer points before performing the optimisation, because the unreachable targets were declared as invalid targets during the optimisation procedure. Additionally, the maximum limit of achievable chromaticity targets cannot be estimated directly. Some targets may not be reached within the gamut due to the number of channels and target luminance. Therefore, we decided to consider all chromaticity targets for optimisation and flag non-achievable targets through the optimisation procedure itself, if no spectrum was found.

The threshold condition of the chromaticity targets was defined with $\Delta u'$, $\Delta v' \leq 5{\times}10^{-5}$ and the luminance L of the optimised spectra was restricted with $\Delta L \leq 1$ cd/m^2. Thus, we define in the following metamer spectra as those that have a maximum distance of $\Delta u'v' \leq 7.05{\times}10^{-5}$ from a target chromaticity coordinate and do

not have a luminance deviation greater than 1 cd/m^2. The implementation of the custom metamer optimisation approach will not be described here as it is part of an upcoming publication. However, metamer spectra can also be optimised using gradient-based or classical black-box heuristic optimisation approaches, as discussed in recent works [58,61,91,98–101]. Through the optimisation, metamer spectra for 473.2 ±SD 18.83 of the 561 given chromaticity targets (Figure 2a, Figure S3) were found on average for each channel configuration and luminance levels (Table S2). We have summarised the descriptive values about the optimisation results in the Supplementary Materials (Table S2). In total, we optimised 1.238521 million spectra across the optimisation targets (Figure S1). The optimised spectra were filtered with a colour rendition condition of CRI $R_a > 80$, from which 1.066843 million remained. Figure 3 shows the melanopic radiance $L_{Mel,\,i}$ against *Duv* from Planckian locus for each CCT in a scatter plot with the CRI > 80 condition. As expected, a higher CCT corresponds to a higher melanopic radiance $L_{Mel,\,i}$, which increases with the luminance level. In principle, a higher melanopic excitation can be achieved for higher colour temperatures by being on and above the Planckian locus, which is caused by the CRI condition. If all optimised spectra are taken into account, irrespective of the colour rendition, the highest melanopic radiance levels can be achieved for CCTs between 6000 and 7443 K at chromaticity coordinates below Planck (Table S1). The number of channels has an advantage at higher CCTs, as one can move further away from Planck while maintaining a certain melanopic radiance level $L_{Mel,\,i}$ and fulfilling the CRI condition (Figure 3). At lower CCTs, the highest melanopic radiance can be achieved below the Planckian locus (Figure 3), whereby a higher number of channels provide more choice of spectra with different melanopic radiance levels. This effect can also be related to the CRI condition. Therefore, a higher number of channels provides more freedom to be off-Planck and maintain the defined criteria of colour fidelity.

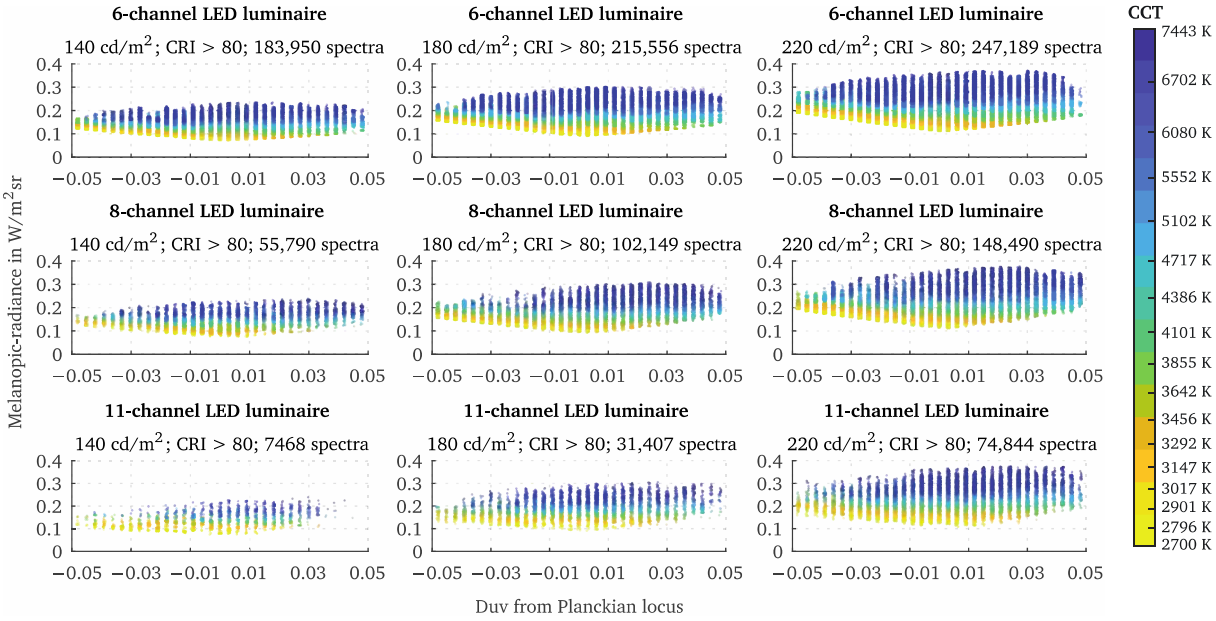

Figure 3. Scatter plot of all optimised spectra's melanopic radiance against *Duv* with a jitter of 0.0005 and a colour rendition condition of CRI $R_a > 80$. A negative *Duv* denotes the chromaticity coordinates below the Planckian locus. As expected, a higher correlated colour temperature can be associated with a stronger circadian response due to the increased proportion in the short wavelength range. However, with increasing *Duv* a higher melanopic radiances can be achieved with CCTs in a range between 2700 to 3456 K. At higher CCTs, a slight decrease in the melanopic radiance can be observed with the 6-channel configuration, mainly caused by the CRI condition. By adding additional LED-channels, one can be more off-Planck while maintaining the melanopic effectiveness. At low CCTs, spectra with chromaticity coordinates below Planck can achieve a higher melanopic level.

In Figure 3, all spectra were considered together, meaning that no distinction was made between metamer spectra $\{X_i(\lambda)\}_{i=1}^{N}$ that have the same ($\Delta u'v' \leq 7.05 \times 10^{-5}$) chromaticity coordinates. For instance, at a luminance of 140 cd/m^2, we found on average for each chromaticity target 445.73 ±SD 430.38 metamers with 6-channels, 169.99 ±SD 112.07 metamers with 8-channels, and 30.29 ±SD 22.19 metamers with 11-channel LEDs. Due to the loop optimisation, there is the possibility of duplicate spectra in the data sets. However, as we were mainly interested in the maximum melanopic metamer contrast, it did not propagate any issues. The number of found metamers differs for each chromaticity target and luminance level between the channel configurations (Table S1). If all found metamer spectra $M_M = [X_1(\lambda),\ X_2(\lambda),\ \ldots,\ X_N(\lambda)]$ for a single chromaticity target at a constant luminance are considered, the spectra with a minimum metamer melanopic radiance $L_{Mel,\ min}$ and maximum metamer radiance $L_{Mel,\ min}$ can be calculated. The melanopic radiance difference between $L_{Mel,\ max}$ and $L_{Mel,\ max}$ with $\Delta L_{Mel,\ max} = L_{Mel,\ max} - L_{Mel,\ min}$ for M_M indicates to what extent the ipRGCs can be modulated at a constant chromaticity coordinate and luminance. In the following, we state the maximum melanopic metamer contrast in per cent with $\Delta \hat{L}_{Mel,\ max} = (100 \times L_{Mel,\ max}/L_{Mel,\ min}) - 100$ to check whether the luminance level could impact the relative melanopic contrast.

In Figure 4a we determined for each chromaticity target the spectrum with the melanopic radiance $L_{Mel,\ max}$ and $L_{Mel,\ min}$ to calculate the maximum melanopic contrast $\Delta \hat{L}_{Mel,\ max}$ between 2700 and 7443 K separately for every *Duv* from the Planckian locus. The calculation of the total contrast between 2700 and 7443 K has shown that the maximum melanopic radiance contrast can be achieved near the Planckian locus (Figure 4a). For instance, the mean value of the maximum relative melanopic contrast for all luminance's using a 6-channel luminaire is 224.80% ±SD 3.59% at a *Duv* between 0 to 0.003 (Figure 4a). In both the 6 and 8 channel configurations, the maximum melanopic contrast between 2700 and 7443 K is less affected by luminance (Figure 4a). For the 11-channel luminaire, the relative melanopsin contrast between 2700 and 7443 K is influenced by the luminance, probably because fewer optimisation results were found at low luminance. Such an effect could be caused by the fact that at low luminance, not all channels can be involved in reaching a certain optimisation target, leading to a reduced number of metamer spectra for each chromaticity target (Figure 3). This could be why more metamers were found with the 11-channel luminaire at 220 cd/m^2 than with the lower luminance levels 140 cd/m^2 and 180 cd/m^2.

In Figure 4b we have calculated the maximum melanopic metamer contrast $\Delta \hat{L}_{Mel,\ max}$ for M_M, representing the percentage by which the ipRGCs can dynamically be triggered at a constant chromaticity coordinate and luminance. The peak melanopic metamer contrast $\Delta \hat{L}_{Mel,\ max}$ was 65.9% and achieved with the 8-channel luminaire configuration at 220 cd/m^2 (*Duv* 0.003), using a CCT of 3855 K (Figure 4b, Table S2). The contrast of the 8-channel and 11-channel luminaire configurations is dependent on the luminance because a higher number of channels, more metamers can be found at higher radiance. For instance, the peak $\Delta \hat{L}_{Mel,\ max}$ across all *Duv*'s and luminance levels range from 55.22 to 58.28% when using the 6-channel configuration, indicating that all LED-channels were used efficiently at 140 cd/m^2, 180 cd/m^2, and 220 cd/m^2 for calculating metamers at the optimisation targets (Figure 4b, Table S2). In comparison, the maximum peak of $\Delta \hat{L}_{Mel,\ max}$ across the luminance levels for the 11-channel luminaire showed a higher dynamic range of 49.16% (140 cd/m^2) to 62.66% (220 cd/m^2). The most significant relative contrast was found at 220 cd/m^2, with which the most metamers were generated by the 11-channel luminaire (Figure 3). With additional LED-channels, it is possible to achieve a higher melanopic metamer contrast with chromaticity targets above the Planckian locus. The CRI condition can be maintained longer with increasing *Duv*, allowing a higher degree of freedom in selecting target chromaticity coordinates. The scatter plot with the absolute melanopic radiance values for the metamer spectra can be found in the Supplementary Materials (Figure S2). Regardless of the luminaire's channel count, it can be observed that the peak melanopic metamer contrast of $\Delta \hat{L}_{Mel,\ max}$ ranges from 49.16 to 65.85% (Figure 4b) and can

be achieved with CCTs between 3292 K and 4717 K, close to the Planckian locus within a *Duv* range of -0.009 to 0.006 (Table S2). Compared to the maximum relative contrast between 2700 K and 7443 K with 234.4% (11-channel, *Duv* 0.006, 220 cd/m^2) (Figure 4a), the melanopic metamer contrast seems to be a powerful tool for triggering the ipRGCs without changing image-forming metrics.

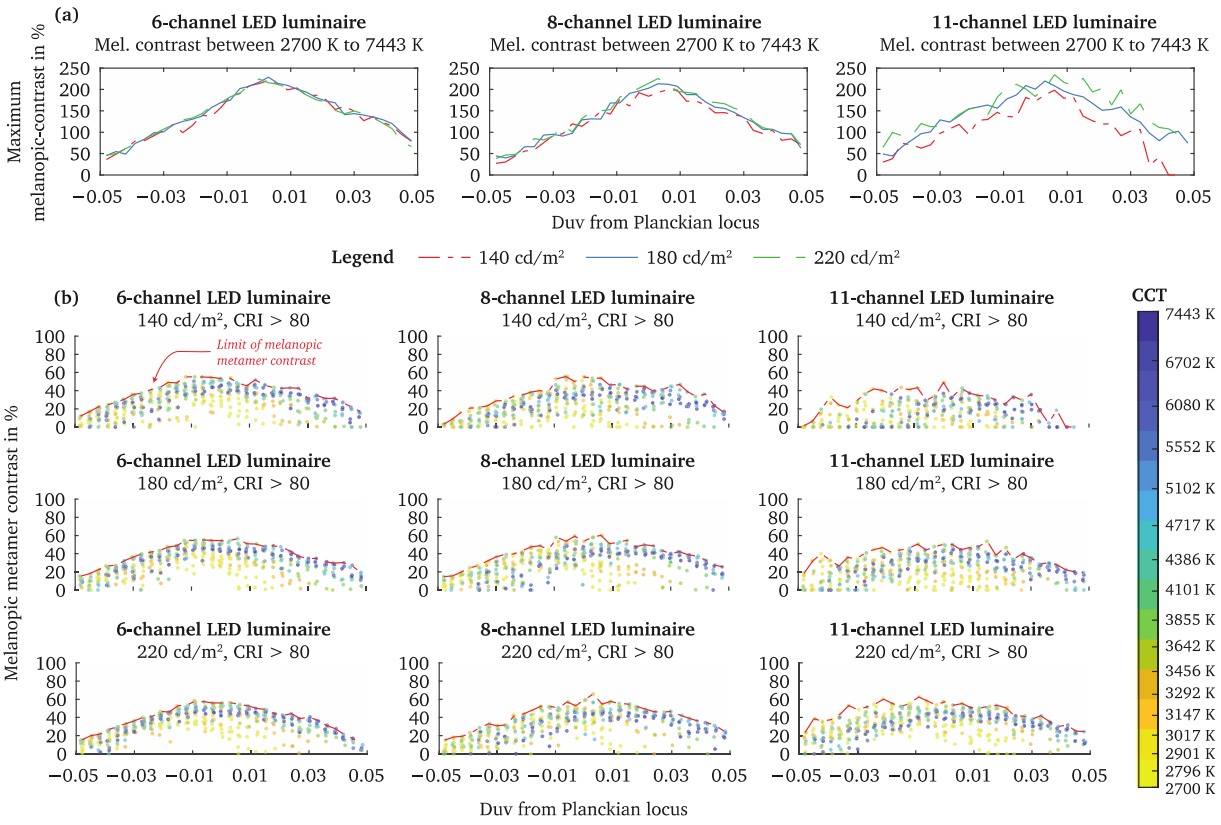

Figure 4. Results for the calculated relative melanopic contrast from the optimised spectra. (**a**) Maximum relative melanopic contrast was calculated between 2700 and 7443 K at constant *Duv* values to the Planckian locus. (**b**) Maximum possible melanopic metamer contrast $\Delta\hat{L}_{Mel,\,max}$ for M_M at a constant chromaticity coordinate within $\Delta u'v' \leq 7.05\times10^{-5}$. The highest relative metamer contrasts for the melanopic radiance can be achieved with chromaticity coordinates near the Planckian locus. By increasing the number of channels, a higher melanopic radiance contrast can be achieved above Planck.

4. Discussion

Previous works already showed that metamer spectra could be used to affect physiological responses [23,66]. For the practical implementation of metamer spectra, it is essential to use stimuli with a high dynamic in their melanopic radiance at a steady chromaticity target. By using 1.2 million optimised spectra, we have found that metamers can reach a relative change in the melanopic radiance between 49.16 to 65.85%. The highest melanopic metamer contrasts were found near the Planckian locus with CCTs between 3292 K and 4717 K. A 6-channel LED luminaire was already sufficient to achieve a relative melanopic contrast of 58.28%. The advantage of using a higher number of LED-channels could be in the degree of freedom to choose chromaticity coordinates above Planck while achieving a higher melanopic radiance compared to a 6-channel configuration. However, we can state that using an 8-channel or 11-channel luminaire does affect the maximum melanopic metamer contrast, but its benefit does not outweigh the effort and costs of a higher channel count. Basically, the limitation of melanopic radiance is caused by the CRI condition. Thus, multi-channel luminaires have the advantage of varying visual metrics while maintaining circadian effectiveness. In this context, the work of Saw et al. recently recommended that at least 4 to 5 LED channels are enough to achieve an optimal balance between colour fidelity

and circadian tunability [61]. Our results also reveal such a tendency, which is why we can conclude that an 8-channel or 11-channel luminaire does not have a significant advantage for non-visual lighting purposes. However, it should be noted that we used the CRI as a colour quality condition without incorporating additional metrics. For instance, using the TM30-15 metric could narrow down the possible metamer contrast. Furthermore, we choose a quite conservative criterion in defining a metamer spectrum, since its chromaticity coordinate was not allowed to deviate more than $\Delta u'v' \leq 7.05 \times 10^{-5}$. In reality, such tolerances are not possible due to temperature fluctuations of the LEDs or measurement inaccuracies, so it can be assumed that with a larger tolerance, the melanopic metamer contrasts should possibly increase.

From our analysis, we can deduce to what extent the relative melanopic radiance contrast can be increased at a constant chromaticity coordinate, but whether this would be sufficient enough for a circadian response was not worked out in our analysis. Although the melanopic radiance or the melanopic irradiance can be utilised as a circadian indicator, it would be useful to evaluate the effect of metamer spectra using advanced circadian models [80,102,103]. Metamers are gaining attention, and studies about such spectra's practical benefits for office lighting are rare. The most important studies about the practical aspects of metamers are from Vethe et al. [23], Allen et al. [66] and Souman et al. [104], revealing that the melanopic contrast of metamer spectra could be high enough to affect the circadian responses. In this context, a recent study [105] optimised six spectra and reported that the circadian stimulus proposed by Rea et al. [103] could be varied from 0.2 to 0.4 while maintaining a similar percept white light ton.

Nevertheless, our large-scale spectral optimisation databases proposed in this work offer the advantage that a more comprehensive analysis can be performed to explore the limits of metamer spectra along the Planckian locus, which was unknown before. While we report that 6-channels are already sufficient to achieve a high melanopic contrast, we did not consider a fewer channel count in our optimisation study. Note, that we have optimised the spectra with different channel configurations; however, the given channel number is the upper limit of what could be used to generate the spectra in the optimisation pipeline. For instance, the 6-channel data set may also include spectra that were generated using 3 LED channels. For an extended evaluation, it would be interesting to classify the data sets according to the active number of channels, to make a refined statement about the efficient number of LED channels for reaching a specific melanopic contrast using metamers.

5. Conclusions

The circadian impact of indoor lighting is affected by the spectral composition, the illumination level and the light intervention timing. Recent studies showed that light intervention in the morning and night could significantly affect the physiological responses [106] and subjective sleepiness ratings [107–111]. However, circadian photoentrainment studies with humans are not consistent, and differences can be found about the extent to which targeted lighting interventions during the day can induce physiological effects [112]. Overall, integrative interior lighting should consider both the imaging and non-imaging visual pathways [113]. An essential perspective in this context is that the visual preferences in indoor lighting and the circadian light sensitivity can differ between individuals [3,74,75,78]. Therefore, personalised interior lighting concepts that employ neural networks to adapt to the user's visual preferences will probably become more essential for practical implementation [78]. Multi-channel LED luminaires provide significant advantages for future smart lighting concepts and will probably play a dominant role due to their spectral flexibility. Recent works did not propose a concept of how individual visual preferences and non-visual lighting effects can be linked in a personalised smart lighting system using a multi-channel LED setup. We proposed that visual metrics should be adjustable by the users' in order to train a non-parametric self-learning lighting system for time-variant light recommendations. The circadian effectiveness of a light setting should be varied via predefined non-visual response models by using metamer spectra only. Such a self-learning lighting

concept could cover a user's visual preference while triggering the non-image-forming pathway through metamer spectra automatically.

The practical implementation of a self-learning system requires a so-called base-user model that needs to be developed using neural networks. For this purpose, connected multi-channel LED luminaires should be placed in office facilities to record the users' light setting and train the non-parametric model. Due to the neural networks' capability of pattern recognition, light preferences can then be recommended that were not present in the training set. Such an advantage is also the biggest hurdle in the technological implementation of the proposed personalised illumination system, as a look-up table can no longer be used to determine the channel values from the luminaire. Suppose a simple scenario in which a trained neural network can recommend the user's preferred light metrics like the chromaticity coordinates and luminance at a given time. In such a case, the predicted light metric setting needs to be adjusted on the luminaire by optimising the respective channel values (Figure 1). Usually, heuristic optimisation is employed for such a task, but they are neither capable of real-time calculations nor scalable for office buildings. Thus, before implementing a personalised smart-lighting system, a necessary step is to develop a scalable spectral optimisation method, capable of adjusting the luminaires' channel values in real-time from light metric recommendations.

Tang et al. [114] developed a real-time optimisation procedure for multi-channel LED luminaires, but the procedure cannot optimise metamer spectra. Therefore, the key technology for implementing our proposed smart lighting system is a real-time spectral black-box optimisation framework, featuring the calculating metamer spectra from any visual lighting metrics. Such a metamer optimisation method for real-time applications does currently not exist. However, the approach of Tang et al. seems to be promising as a starting point for such a missing real-time metamer optimiser, as it evens works on a mobile phone.

In addition to the technological aspects, it is crucial to determine how many channels and which LED combinations are required for reaching the maximum melanopic contrast with metamer spectra across the entire Planckian locus. Previous works have taken the approach of optimising metamer spectra for individual chromaticity coordinates. Assuming that the user is free to vary the chromaticity coordinate in a smart lighting system, metamer spectra must be computable across the Planckian locus. Here we have chosen the technique of optimising metamer spectra at a large scale to comprehend the pattern of metamer spectra against the melanopic radiance for the first time.

Compared to previous spectral optimisation studies [6,58,60–63,100,101,115–118], this work provides at the authors' best knowledge one of the most comprehensive multichannel LED datasets for metamer spectra. More advanced analyses between additional colour quality metrics are possible with the optimised spectra, which we did not fully exploit. The significant effort in this work was the optimisation of the spectra for the 561 chromaticity targets at three different luminance levels and three LED channel configurations. Therefore, we publish with this work over 1.2 million spectra in an open-source repository, allowing other research groups to carry out extended calculations. Note that there may be duplicate spectra in the data set because the optimisation was performed in a loop for finding an appropriate number of metamers. In analyses where repeated spectra could affect the results, a pre-filtering must be performed.

As a next step, we are working on an upgrade of this dataset to provide a higher number of metamer spectra, generated with an additional count of LED-channel combinations. Such a database could support the selection and combination of LEDs in multi-channel systems, as repeated optimisations of individual combinations are currently necessary to make recommendations in indoor lighting.

Supplementary Materials: The optimized spectra are available online at https://github.com/BZandi/MDPI-Smart-Lighting-Spectra. Figure S1: Scatter plot of the melanopic radiance against *Duv* for optimised spectra without a CRI condition, Table S1: Number of spectra which were generated for each chromaticity target, Table S2: Values of maximum possible melanopic metamer contrast

dependent on the used channel configuration and luminance, Figure S2: Scatter plot of maximum possible melanopic metamer contrast in W/m^2sr. Figure S3: Illustration of the CIExy-2° chromaticity targets for which spectra were successfully optimised.

Author Contributions: Conceptualization, B.Z. and T.Q.K.; methodology, B.Z., A.E., and A.H.; software, B.Z.; validation, B.Z.; formal analysis, B.Z.; data curation, B.Z.; writing—original draft preparation, B.Z.; writing—review and editing, B.Z., A.E., A.H. and T.Q.K.; visualization, B.Z.; project administration, B.Z. and T.Q.K.; funding acquisition, T.Q.K. All authors have read and agreed to the published version of the manuscript.

Funding: This research was funded by the Deutsche Forschungsgemeinschaft (DFG, German Research Foundation)–450636577.

Acknowledgments: The calculations in this work were performed on the Lichtenberg high-performance computer of the Technical University of Darmstadt. The authors would like to thank the Hessian Competence Centre for High Performance Computing funded by the Hessen State Ministry of Higher Education, Research and the Arts. We acknowledge support by the German Research Foundation and the Open Access Publishing fund of the Technical University of Darmstadt. We thank Katherine Anne Chatziannidou for proofreading this work.

Conflicts of Interest: The authors declare no conflict of interest. The funder had no role in the design of the study; in the collection, analyses, or interpretation of data; in the writing of the manuscript, or in the decision to publish the results.

References

1. Bodmann, H.W. Elements of photometry, brightness and visibility. *Light Res. Technol.* **1992**, *24*, 29–42. [CrossRef]
2. Sharpe, L.T.; Stockman, A.; Jagla, W.; Jaägle, H. A luminous efficiency function, V*(λ), for daylight adaptation. *J. Vis.* **2005**, *5*, 948–968. [CrossRef]
3. Tan, F.; Caicedo, D.; Pandharipande, A.; Zuniga, M. Sensor-Driven, human-in-the-loop lighting control. *Light Res. Technol.* **2018**, *50*, 660–680. [CrossRef]
4. Kingdom, F.A.A.; Mullen, K.T. Separating colour and luminance information in the visual system. *Spat. Vis.* **1995**, *9*, 191–219. [CrossRef] [PubMed]
5. Jennings, B.J.; Martinovic, J. Luminance and color inputs to mid-level and high-level vision. *J. Vis.* **2014**, *14*, 1–17. [CrossRef] [PubMed]
6. Oh, J.H.; Yang, S.J.; Do, Y.R. Healthy, natural, efficient and tunable lighting: Four-Package white LEDs for optimizing the circadian effect, color quality and vision performance. *Light Sci. Appl.* **2014**, *3*, e141. [CrossRef]
7. Chew, I.; Kalavally, V.; Tan, C.P.; Parkkinen, J. A spectrally tunable smart LED lighting system with closed-loop control. *IEEE Sens. J.* **2016**, *16*, 4452–4459. [CrossRef]
8. Fernanádez-Montes, A.; Gonzalez-Abril, L.; Ortega, J.A.; Morente, F.V. A study on saving energy in artificial lighting by making smart use of wireless sensor networks and actuators. *IEEE Netw.* **2009**, *23*, 16–20. [CrossRef]
9. Matta, S.; Mahmud, S.M. An intelligent light control system for power saving. In Proceedings of the IECON 2010—36th Annual Conference on IEEE Industrial Electronics Society, Glendale, AZ, USA, 7–10 November 2010; pp. 3316–3321. [CrossRef]
10. Chew, I.; Kalavally, V.; Oo, N.W.; Parkkinen, J. Design of an energy-saving controller for an intelligent LED lighting system. *Energy Build.* **2016**, *120*, 1–9. [CrossRef]
11. Von Neida, B.; Manicria, D.; Tweed, A. An analysis of the energy and cost savings potential of occupancy sensors for commercial lighting systems. *J. Illum. Eng. Soc.* **2001**, *30*, 111–125. [CrossRef]
12. Kompier, M.E.; Smolders, K.C.H.J.; de Kort, Y.A.W. A systematic literature review on the rationale for and effects of dynamic light scenarios. *Build. Environ.* **2020**, *186*, 107326. [CrossRef]
13. Stefani, O.; Freyburger, M.; Veitz, S.; Basishvili, T.; Meyer, M.; Weibel, J.; Kobayashi, K.; Shirakawa, Y.; Cajochen, C. Changing color and intensity of LED lighting across the day impacts on circadian melatonin rhythms and sleep in healthy men. *J. Pineal. Res.* **2020**. [CrossRef]
14. Hattar, S. Melanopsin-Containing retinal ganglion cells: Architecture, projections, and intrinsic photosensitivity. *Science* **2002**, *295*, 1065–1070. [CrossRef] [PubMed]
15. Gooley, J.J.; Lu, J.; Chou, T.C.; Scammell, T.E.; Saper, C.B. Melanopsin in cells of origin of the retinohypothalamic tract. *Nat. Neurosci.* **2001**, *4*, 1165. [CrossRef] [PubMed]
16. Provencio, I.; Rodriguez, I.R.; Jiang, G.; Hayes, W.P.; Moreira, E.F.; Rollag, M.D. A novel human opsin in the inner retina. *J. Neurosci.* **2000**, *20*, 600–605. [CrossRef]
17. Provencio, I.; Jiang, G.; De Grip, W.J.; Pär Hayes, W.; Rollag, M.D. Melanopsin: An opsin in melanophores, brain, and eye. *Proc. Natl. Acad. Sci. USA* **1998**, *95*, 340–345. [CrossRef]
18. Berson, D.M.; Dunn, F.A.; Takao, M. Phototransduction by retinal ganglion cells that set the circadian clock. *Science* **2002**, *295*, 1070–1073. [CrossRef]

19. Zandi, B.; Guo, X.; Bodrogi, P.; Khanh, T.Q. Experimental evaluation of different brightness perception models based on human pupil light responses. In Proceedings of the CIE 2018 "Topical Conference on Smart Lighting", Taipei, Taiwan, 26–27 April 2018; Volume 2, pp. 201–208. [CrossRef]
20. Münch, M.; Wirz-Justice, A.; Brown, S.A.; Kantermann, T.; Martiny, K.; Stefani, O.; Vetter, C.; Wright, K.P., Jr.; Wulff, K.; Skene, D.J. The role of daylight for humans: Gaps in current knowledge. *Clocks Sleep* **2020**, *2*, 61–85. [CrossRef]
21. Cajochen, C.; Münch, M.; Kobialka, S.; Kräuchi, K.; Steiner, R.; Oelhafen, P.; Orgul, S.; Wirz-Justice, A. High sensitivity of human melatonin, alertness, thermoregulation, and heart rate to short wavelength light. *J. Clin. Endocrinol. Metab.* **2005**, *90*, 1311–1316. [CrossRef]
22. Pauley, S.M. Lighting for the human circadian clock: Recent research indicates that lighting has become a public health issue. *Med. Hypotheses* **2004**, *63*, 588–596. [CrossRef]
23. Vethe, D.; Scott, J.; Engstrøm, M.; Salvesen, Ø.; Sand, T.; Olsen, A.; Morken, G.; Heglum, H.S.; Kjørstad, K.; Faaland, P.M.; et al. The evening light environment in hospitals can be designed to produce less disruptive effects on the circadian system and improve sleep. *Sleep* **2020**, 1–12. [CrossRef]
24. Lee, S.K.; Sonoda, T.; Schmidt, T.M. M1 intrinsically photosensitive retinal ganglion cells integrate rod and melanopsin inputs to signal in low light. *Cell Rep.* **2019**, *29*, 3349–3355. [CrossRef] [PubMed]
25. Do, M.T.H.; Yau, K.W. Adaptation to steady light by intrinsically photosensitive retinal ganglion cells. *Proc. Natl. Acad. Sci. USA* **2013**, *110*, 7470–7475. [CrossRef] [PubMed]
26. Schmidt, T.M.; Chen, S.; Hattar, S. Intrinsically photosensitive retinal ganglion cells: Many subtypes, diverse functions. *Trends Neurosci.* **2011**, *34*, 572–580. [CrossRef] [PubMed]
27. Quattrochi, L.E.; Stabio, M.E.; Kim, I.; Ilardi, M.C.; Fogerson, P.M.; Leyrer, M.L.; Berson, D.M. The M6 cell: A small-field bistratified photosensitive retinal ganglion cell. *J. Comp. Neurol.* **2019**, *527*, 297–311. [CrossRef]
28. Zhao, X.; Stafford, B.K.; Godin, A.L.; King, W.M.; Wong, K.Y. Photoresponse diversity among the five types of intrinsically photosensitive retinal ganglion cells. *J. Physiol.* **2014**, *592*, 1619–1636. [CrossRef]
29. Stabio, M.E.; Sabbah, S.; Quattrochi, L.E.; Ilardi, M.C.; Fogerson, P.M.; Leyrer, M.L.; Kim, M.T.; Kim, I.; Schiel, M.; Renna, J.M.; et al. The M5 cell: A color-opponent intrinsically photosensitive retinal ganglion cell. *Neuron* **2018**, *97*, 251. [CrossRef]
30. Bonmati-Carrion, M.A.; Hild, K.; Isherwood, C.; Sweeney, S.J.; Revell, V.L.; Skene, D.J.; Rol, M.A.; Madrid, J.A. Relationship between human pupillary light reflex and circadian system status. *PLoS ONE* **2016**, *11*, e0162476. [CrossRef]
31. Fernandez, D.C.; Fogerson, P.M.; Ospri, L.L.; Thomsen, M.B.; Layne, R.M.; Severin, D.; Zhan, J.; Singer, J.H.; Kirkwood, A.; Zhao, H.; et al. Light affects mood and learning through distinct retina-brain pathways. *Cell* **2018**, *175*, 71–84.e18. [CrossRef]
32. Beier, C.; Zhang, Z.; Yurgel, M.; Hattar, S. The projections of ipRGCs and conventional RGCs to retinorecipient brain nuclei. *BioRxiv* **2020**. [CrossRef]
33. Lucas, R.J.; Hattar, S.; Takao, M.; Berson, D.M.; Foster, R.G.; Yau, K.W. Diminished pupillary light reflex at high irradiances in melanopsin-knockout mice. *Science* **2003**, *299*, 245–247. [CrossRef] [PubMed]
34. Ecker, J.L.; Dumitrescu, O.N.; Wong, K.Y.; Alam, N.M.; Chen, S.-K.; LeGates, T.; Renna, J.M.; Prusky, G.T.; Berson, D.M.; Hattar, S. Melanopsin-Expressing retinal ganglion-cell photoreceptors: Cellular diversity and role in pattern vision. *Neuron* **2010**, *67*, 49–60. [CrossRef] [PubMed]
35. Do, M.T.H.; Kang, S.H.; Xue, T.; Zhong, H.; Liao, H.W.; Bergles, D.E.; Yau, K.-W. Photon capture and signalling by melanopsin retinal ganglion cells. *Nature* **2009**, *457*, 281–287. [CrossRef] [PubMed]
36. Hattar, S.; Kumar, M.; Park, A.; Tong, P.; Tung, J.; Yau, K.-W.; Berson, D.M. Central projections of melanopsin-expressing retinal ganglion cells in the mouse. *J. Comp. Neurol.* **2006**, *497*, 326–349. [CrossRef]
37. Zandi, B.; Khanh, T.Q. Deep learning-based pupil model predicts time and spectral dependent light responses. *Sci. Rep.* **2021**, *11*, 841. [CrossRef]
38. Grünert, U.; Jusuf, P.R.; Lee, S.C.S.; Nguyen, D.T. Bipolar input to melanopsin containing ganglion cells in primate retina. *Vis. Neurosci.* **2011**, *28*, 39–50. [CrossRef]
39. Patterson, S.S.; Kuchenbecker, J.A.; Anderson, J.R.; Neitz, M.; Neitz, J. A color vision circuit for non-image-forming vision in the primate retina. *Curr. Biol.* **2020**, *30*, 1269–1274.e2. [CrossRef]
40. Yamakawa, M.; Tsujimura, S.; Okajima, K. A quantitative analysis of the contribution of melanopsin to brightness perception. *Sci. Rep.* **2019**, *9*, 1–8. [CrossRef]
41. Dacey, D.M.; Liao, H.-W.; Peterson, B.B.; Robinson, F.R.; Smith, V.C.; Pokorny, J.; Yau, K.-W.; Gamlin, P.D. Melanopsin-Expressing ganglion cells in primate retina signal colour and irradiance and project to the LGN. *Nature* **2005**, *433*, 749–754. [CrossRef]
42. Wong, K.Y.; Dunn, F.A.; Graham, D.M.; Berson, D.M. Synaptic influences on rat ganglion-cell photoreceptors. *J. Physiol.* **2007**, *582*, 279–296. [CrossRef]
43. Zandi, B.; Klabes, J.; Khanh, T.Q. Prediction accuracy of L- and M-cone based human pupil light models. *Sci. Rep.* **2020**, *10*, 10988. [CrossRef] [PubMed]
44. Cao, D.; Nicandro, N.; Barrionuevo, P.A. A five-primary photostimulator suitable for studying intrinsically photosensitive retinal ganglion cell functions in humans. *J. Vis.* **2015**, *15*, 1–13. [CrossRef] [PubMed]
45. Spitschan, M.; Jain, S.; Brainard, D.H.; Aguirre, G.K. Opponent melanopsin and S-cone signals in the human pupillary light response. *Proc. Natl. Acad. Sci. USA* **2014**, *111*, 15568–15572. [CrossRef] [PubMed]

46. Allen, A.E.; Brown, T.M.; Lucas, R.J. A distinct contribution of short-wavelength-sensitive cones to light-evoked activity in the mouse pretectal olivary nucleus. *J. Neurosci.* **2011**, *31*, 16833–16843. [CrossRef]
47. Göz, D.; Studholme, K.; Lappi, D.A.; Rollag, M.D.; Provencio, I.; Morin, L.P. Targeted destruction of photosensitive retinal ganglion cells with a saporin conjugate alters the effects of light on mouse circadian rhythms. *PLoS ONE* **2008**, *3*, e3153. [CrossRef] [PubMed]
48. Güler, A.D.; Ecker, J.L.; Lall, G.S.; Haq, S.; Altimus, C.M.; Liao, H.W.; Barnard, A.R.; Cahill, H.; Badea, T.C.; Zhao, H.; et al. Melanopsin cells are the principal conduits for rod-cone input to non-image-forming vision. *Nature* **2008**, *453*, 102–105. [CrossRef]
49. Hatori, M.; Le, H.; Vollmers, C.; Keding, S.R.; Tanaka, N.; Schmedt, C.; Jegla, T.; Panda, S. Inducible ablation of melanopsin-expressing retinal ganglion cells reveals their central role in non-image forming visual responses. *PLoS ONE* **2008**, *3*, e2451. [CrossRef]
50. Altimus, C.M.; Güler, A.D.; Villa, K.L.; McNeill, D.S.; LeGates, T.A.; Hattar, S. Rods-Cones and melanopsin detect light and dark to modulate sleep independent of image formation. *Proc. Natl. Acad. Sci. USA* **2008**, *105*, 19998–20003. [CrossRef]
51. LeGates, T.A.; Altimus, C.M.; Wang, H.; Lee, H.K.; Yang, S.; Zhao, H.; Kirkwood, A.; Weber, E.T.; Hattar, S. Aberrant light directly impairs mood and learning through melanopsin-expressing neurons. *Nature* **2012**, *491*, 594–598. [CrossRef]
52. Rupp, A.C.; Ren, M.; Altimus, C.M.; Fernandez, D.C.; Richardson, M.; Turek, F.; Hattar, S.; Schmidt, T.M. Distinct ipRGC subpopulations mediate light's acute and circadian effects on body temperature and sleep. *eLife* **2019**, *8*. [CrossRef]
53. Brown, T.M. Melanopic illuminance defines the magnitude of human circadian light responses under a wide range of conditions. *J. Pineal. Res.* **2020**, 1–14. [CrossRef] [PubMed]
54. Lucas, R.J.; Peirson, S.N.; Berson, D.M.; Brown, T.M.; Cooper, H.M.; Czeisler, C.A.; Figueiro, M.G.; Gamlin, P.D.; Lockley, S.W.; O'Hagan, J.B.; et al. Measuring and using light in the melanopsin age. *Trends Neurosci.* **2014**, *37*, 1–9. [CrossRef] [PubMed]
55. CIE. CIE S 026/E:2018. In *CIE System for Metrology of Optical Radiation for ipRGC-Influenced Responses to Light*; CIE: Vienna, Austria, 2018. [CrossRef]
56. Schmidt, T.M.; Kofuji, P. Functional and morphological differences among intrinsically photosensitive retinal ganglion cells. *J. Neurosci.* **2009**, *29*, 476–482. [CrossRef]
57. McDougal, D.H.; Gamlin, P.D. The influence of intrinsically-photosensitive retinal ganglion cells on the spectral sensitivity and response dynamics of the human pupillary light reflex. *Vision Res.* **2010**, *50*, 72–87. [CrossRef] [PubMed]
58. Afshari, S.; Moynihan, L.; Mishra, S. An optimisation toolbox for multi-colour LED lighting. *Light Res. Technol.* **2016**, 1–15. [CrossRef]
59. Leike, I. Optimized additive mixing of colored light-emitting diode sources. *Opt. Eng.* **2004**, *43*, 1531. [CrossRef]
60. Soltic, S.; Chalmers, A. Optimization of LED lighting for clinical settings. *J. Healthc. Eng.* **2019**, *2019*. [CrossRef]
61. Saw, Y.J.; Kalavally, V.; Tan, C.P. The spectral optimization of a commercializable multi-channel LED panel with circadian impact. *IEEE Access* **2020**, *8*, 136498–136511. [CrossRef]
62. Dai, Q.; Shan, Q.; Lam, H.; Hao, L.; Lin, Y.; Cui, Z. Circadian-Effect engineering of solid-state lighting spectra for beneficial and tunable lighting. *Opt. Express* **2016**, *24*, 20049. [CrossRef]
63. Zhang, J.; Guo, W.; Xie, B.; Yu, X.; Luo, X.; Zhang, T.; Yu, Z.; Wang, H.; Jin, X. Blue light hazard optimization for white light-emitting diode sources with high luminous efficacy of radiation and high color rendering index. *Opt. Laser Technol.* **2017**, *94*, 193–198. [CrossRef]
64. Spitschan, M.; Woelders, T. The method of silent substitution for examining melanopsin contributions to pupil control. *Front. Neurol.* **2018**, *9*. [CrossRef] [PubMed]
65. Finlayson, G.; Mackiewicz, M.; Hurlbert, A.; Pearce, B.; Crichton, S. On calculating metamer sets for spectrally tunable LED illuminators. *J. Opt. Soc. Am.* **2014**, *31*, 1577. [CrossRef] [PubMed]
66. Allen, A.E.; Hazelhoff, E.M.; Martial, F.P.; Cajochen, C.; Lucas, R.J. Exploiting metamerism to regulate the impact of a visual display on alertness and melatonin suppression independent of visual appearance. *Sleep* **2018**, *41*, 1–7. [CrossRef] [PubMed]
67. Hung, S.-M.; Milea, D.; Rukmini, A.V.; Najjar, R.P.; Tan, J.H.; Viénot, F.; Dubail, M.; Tow, S.L.C.; Aung, T.; Gooley, J.J.; et al. Cerebral neural correlates of differential melanopic photic stimulation in humans. *Neuroimage* **2017**, *146*, 763–769. [CrossRef]
68. Cheng, Z.; Zhao, Q.; Wang, F.; Jiang, Y.; Xia, L.; Ding, J. Satisfaction based Q-learning for integrated lighting and blind control. *Energy Build.* **2016**, *127*, 43–55. [CrossRef]
69. Gunay, H.B.; O'Brien, W.; Beausoleil-Morrison, I. A critical review of observation studies, modeling, and simulation of adaptive occupant behaviors in offices. *Build. Environ.* **2013**, *70*, 31–47. [CrossRef]
70. Jennings, J.D.; Rubinstein, F.M.; DiBartolomeo, D.; Blanc, S.L. Comparison of control options in private offices in an advanced lighting controls testbed. *J. Illum. Eng. Soc.* **2000**, *29*, 39–60. [CrossRef]
71. Wang, N.; Phelan, P.E.; Gonzalez, J.; Harris, C.; Henze, G.P.; Hutchinson, R.; Langevin, J.; Lazarus, M.A.; Nelson, B.; Pyke, C.; et al. Ten questions concerning future buildings beyond zero energy and carbon neutrality. *Build. Environ.* **2017**, *119*, 169–182. [CrossRef]
72. Nagy, Z.; Yong, F.Y.; Schlueter, A. Occupant centered lighting control: A user study on balancing comfort, acceptance, and energy consumption. *Energy Build.* **2016**, *126*, 310–322. [CrossRef]
73. Reinhart, C.; Voss, K. Monitoring manual control of electric lighting and blinds. *Light Res. Technol.* **2003**, *35*, 243–258. [CrossRef]
74. Chellappa, S.L. Individual differences in light sensitivity affect sleep and circadian rhythms. *Sleep* **2020**. [CrossRef] [PubMed]

75. Phillips, A.J.K.; Vidafar, P.; Burns, A.C.; McGlashan, E.M.; Anderson, C.; Rajaratnam, S.M.W.; Lockley, S.W.; Cain, S.W. High sensitivity and interindividual variability in the response of the human circadian system to evening light. *Proc. Natl. Acad. Sci. USA* **2019**, *116*, 12019–12024. [CrossRef] [PubMed]
76. Papatsimpa, C.; Linnartz, J.-P. Personalized office lighting for circadian health and improved sleep. *Sensors* **2020**, *20*, 4569. [CrossRef] [PubMed]
77. Wang, Z.; Tan, Y.K. Illumination control of LED systems based on neural network model and energy optimization algorithm. *Energy Build.* **2013**, *62*, 514–521. [CrossRef]
78. Kandasamy, N.K.; Karunagaran, G.; Spanos, C.; Tseng, K.J.; Soong, B.-H. Smart lighting system using ANN-IMC for personalized lighting control and daylight harvesting. *Build. Environ.* **2018**, *139*, 170–180. [CrossRef]
79. Tran, D.; Tan, Y.K. Sensorless illumination control of a networked LED-lighting system using feedforward neural network. *IEEE Trans. Ind. Electron.* **2014**, *61*, 2113–2121. [CrossRef]
80. Truong, W.; Zandi, B.; Trinh, V.Q.; Khanh, T.Q. Circadian metric—Computation of circadian stimulus using illuminance, correlated colour temperature and colour rendering index. *Build. Environ.* **2020**, *184*, 107146. [CrossRef]
81. Chiogna, M.; Mahdavi, A.; Albatici, R.; Frattari, A. Energy efficiency of alternative lighting control systems. *Light Res. Technol.* **2012**, *44*, 397–415. [CrossRef]
82. Hughes, R.F.; Dhannu, S.S. Substantial energy savings through adaptive lighting. In Proceedings of the 2008 IEEE Electric Power Energy Conference, Vancouver, BC, Canada, 6–7 October 2008. [CrossRef]
83. Caicedo, D.; Pandharipande, A. Daylight and occupancy adaptive lighting control system: An iterative optimization approach. *Light Res. Technol.* **2016**, *48*, 661–675. [CrossRef]
84. Seyedolhosseini, A.; Masoumi, N.; Modarressi, M.; Karimian, N. Daylight adaptive smart indoor lighting control method using artificial neural networks. *J. Build. Eng.* **2020**, *29*, 101141. [CrossRef]
85. Sun, F.; Yu, J. Indoor intelligent lighting control method based on distributed multi-agent framework. *Optik (Stuttg.)* **2020**, *213*, 164816. [CrossRef]
86. Wang, Y.; Dasgupta, P. Designing an adaptive lighting control system for smart buildings and homes. In Proceedings of the 2015 IEEE 12th International Conference on Networking, Sensing and Control, Taipei, Taiwan, 9–11 April 2015; pp. 450–455. [CrossRef]
87. Afshari, S.; Mishra, S.; Julius, A.; Lizarralde, F.; Wason, J.D.; Wen, J.T. Modeling and control of color tunable lighting systems. *Energy Build.* **2014**, *68*, 242–253. [CrossRef]
88. Beccali, M.; Bonomolo, M.; Ciulla, G.; Lo Brano, V. Assessment of indoor illuminance and study on best photosensors' position for design and commissioning of Daylight Linked Control systems. A new method based on artificial neural networks. *Energy* **2018**, *154*, 466–476. [CrossRef]
89. Seyedolhosseini, A.; Masoumi, N.; Modarressi, M.; Karimian, N. Zone based control methodology of smart indoor lighting systems using feedforward neural networks. In Proceedings of the 2018 9th International Symposium on Telecommunications (IST), Tehran, Iran, 17–19 December 2018; pp. 201–206. [CrossRef]
90. Cole, R.J.; Brown, Z. Reconciling human and automated intelligence in the provision of occupant comfort. *Intell. Build. Int.* **2009**, *1*, 39–55. [CrossRef]
91. Zhang, F.; Xu, H.; Wang, Z. Spectral design methods for multi-channel LED light sources based on differential evolution. *Appl. Opt.* **2016**, *55*, 7771–7781. [CrossRef]
92. Babilon, S.; Khanh, T.Q. Color appearance rating of familiar real objects under immersive viewing conditions. *Color Res. Appl.* **2018**, *43*, 551–568. [CrossRef]
93. Bodrogi, P.; Guo, X.; Stojanovic, D.; Fischer, S.; Khanh, T.Q. Observer preference for perceived illumination chromaticity. *Color Res. Appl.* **2018**, *43*, 506–516. [CrossRef]
94. Dangol, R.; Islam, M.S.; Hyvärinen, M.; Bhushal, P.; Puolakka, M.; Halonen, L. User acceptance studies for LED office lighting: Preference, naturalness and colourfulness. *Light Res. Technol.* **2015**, *47*, 36–53. [CrossRef]
95. Wang, Y.; Wei, M. Preference among light sources with different Duv but similar colour rendition: A pilot study. *Light Res. Technol.* **2018**, *50*, 1013–1023. [CrossRef]
96. Wei, M.; Houser, K.W. What is the cause of apparent preference for sources with chromaticity below the blackbody locus? *LEUKOS J. Illum. Eng. Soc. N. Am.* **2016**, *12*, 95–99. [CrossRef]
97. Dikel, E.E.; Burns, G.J.; Veitch, J.A.; Mancini, S.; Newsham, G.R. Preferred chromaticity of color-tunable LED lighting. *LEUKOS J. Illum. Eng. Soc. N. Am.* **2014**, *10*, 101–115. [CrossRef]
98. Zhang, F.; Xu, H.; Wang, Z. Optimizing spectral compositions of multichannel LED light sources by IES color fidelity index and luminous efficacy of radiation. *Appl. Opt.* **2017**, *56*, 1962–1971. [CrossRef] [PubMed]
99. Cui, Y.; Geng, Z.; Zhu, Q.; Han, Y. Review: Multi-Objective optimization methods and application in energy saving. *Energy* **2017**, *125*, 681–704. [CrossRef]
100. Dai, Q.; Cai, W.; Hao, L.; Shi, W.; Wang, Z. Spectral optimisation and a novel lighting-design space based on circadian stimulus. *Light Res. Technol.* **2018**, *50*, 1198–1211. [CrossRef]
101. Soltic, S.; Chalmers, A. Differential evolution for the optimisation of multi-band white LED light sources. *Light Res. Technol.* **2012**, *44*, 224–237. [CrossRef]

102. Liu, Y.; Zhixian, Z.; Luo, M.R. The impact and model of CS and CCT on alertness. In Proceedings of the 2020 17th China International Forum on Solid State Lighting & 2020 International Forum on Wide Bandgap Semiconductors China (SSLChina: IFWS); Shenzhen, China: 23–25 November 2020; pp. 196–198. [CrossRef]
103. Rea, M.S.; Figueiro, M.G. Light as a circadian stimulus for architectural lighting. *Light Res. Technol.* **2018**, *50*, 497–510. [CrossRef]
104. Souman, J.L.; Borra, T.; de Goijer, I.; Schlangen, L.J.M.; Vlaskamp, B.N.S.; Lucassen, M.P. Spectral tuning of white light allows for strong reduction in melatonin suppression without changing illumination level or color temperature. *J. Biol. Rhythms* **2018**, *33*, 420–431. [CrossRef]
105. Aderneuer, T.; Stefani, O.; Fernández, O.; Cajochen, C.; Ferrini, R. Circadian tuning with metameric white light: Visual and non-visual aspects. *Light Res. Technol.*. [CrossRef]
106. Van Lieshout-van Dal, E.; Snaphaan, L.; Bongers, I. Biodynamic lighting effects on the sleep pattern of people with dementia. *Build. Environ.* **2019**, *150*, 245–253. [CrossRef]
107. Cajochen, C.; Zeitzer, J.M.; Czeisler, C.A.; Dijk, D.-J. Dose-Response relationship for light intensity and ocular and electroencephalographic correlates of human alertness. *Behav. Brain Res.* **2000**, *115*, 75–83. [CrossRef]
108. Sunde, E.; Pedersen, T.; Mrdalj, J.; Thun, E.; Grønli, J.; Harris, A.; Bjorvatn, B.; Waage, S.; Skene, D.J.; Pallesen, S. Blue-Enriched white light improves performance but not subjective alertness and circadian adaptation during three consecutive simulated night shifts. *Front. Psychol.* **2020**, *11*. [CrossRef] [PubMed]
109. Rahman, S.A.; Wright, K.P.; Lockley, S.W.; Czeisler, C.A.; Gronfier, C. Characterizing the temporal dynamics of melatonin and cortisol changes in response to nocturnal light exposure. *Sci. Rep.* **2019**, *9*, 19720. [CrossRef] [PubMed]
110. Choi, K.; Shin, C.; Kim, T.; Chung, H.J.; Suk, H.-J. Awakening effects of blue-enriched morning light exposure on university students' physiological and subjective responses. *Sci. Rep.* **2019**, *9*, 345. [CrossRef] [PubMed]
111. Blume, C.; Garbazza, C.; Spitschan, M. Effects of light on human circadian rhythms, sleep and mood. *Somnologie* **2019**, *23*, 147–156. [CrossRef] [PubMed]
112. Van Duijnhoven, J.; Aarts, M.; Kort, H. Personal lighting conditions of office workers: An exploratory field study. *Light Res. Technol.* **2020**. [CrossRef]
113. Houser, K.; Boyce, P.; Zeitzer, J.; Herf, M. Human-Centric lighting: Myth, magic or metaphor? *Light Res. Technol.* **2020**. [CrossRef]
114. Tang, S.J.W.; Kalavally, V.; Ng, K.Y.; Tan, C.P.; Parkkinen, J. Real-Time closed-loop color control of a multi-channel luminaire using sensors onboard a mobile device. *IEEE Access* **2018**, *6*, 54751–54759. [CrossRef]
115. Li, H.-C.; Sun, P.-L.; Huang, Y.; Luo, M.R. Spectral optimization of white LED based on mesopic luminance and color gamut volume for dim lighting conditions. *Appl. Sci.* **2020**, *10*, 3579. [CrossRef]
116. Lei, S.-D.; Liu, B.-J.; Gao, Y.; Dong, X.-Y.; Gong, Y.-J.; Xu, J.; Xu, Y.-X.; Wang, D.; Guo, Z.-Q.; Wu, T.-Z.; et al. Investigation on circadian action and color quality in laser-based illuminant for general lighting and display. *IEEE Photonics. J.* **2020**, *12*, 1–9. [CrossRef]
117. Wu, H.; Dong, J.; Qi, G.; Zhang, G. Optimization of LED light spectrum to enhance colorfulness of illuminated objects with white light constraints. *J. Opt. Soc. Am.* **2015**, *32*, 1262. [CrossRef]
118. Abeysekera, S.K.; Kalavally, V.; Ooi, M.; Kuang, Y.C. Impact of circadian tuning on the illuminance and color uniformity of a multichannel luminaire with spatially optimized LED placement. *Opt. Express* **2020**, *28*, 130. [CrossRef] [PubMed]